Chapter 3: Analysis of Dendritic Arborization and Spine Morphology

Introduction

Neurons are specialized computational compartments that integrate and regulate the propagation of information. The principle language used by neurons to communicate with each other is the action potential. Numerous biophysical and structural properties of neurons have evolved to modulate action potential integration and propagation. Cellular morphology is crucial to our understanding of information processing and communication styles, because neuronal shape is directly related to the computations performed by the cell [1]. Two key morphological characteristics of neurons are dendritic arbor structure and dendritic spine geometry. While spines [2] and dendritic branches [3] can both operate as computational compartments, how their shape, size, and structure affect their function and intrinsic properties is still poorly understood.

An astonishing diversity of dendritic arbor structures exists among neurons of different and similar classes (Fig 3.1). The shape, size, and complexity of dendritic trees can modulate action potential propagation [4] and influence the intrinsic firing pattern of a neuron [5]. Specifically, Mainen and Sejnowski demonstrated that firing patterns correlate strongly with the extent of arborization, and Vetter et al. [4] showed that action potential propagation is strongly influenced by 1) the number of branching points, 2) the rate of increase in dendritic membrane area, and 3) the relationship between the diameter of parent and daughter dendrites at branchpoints. Ultimately, both of these studies imply

that the level of dendritic complexity is a key metric for understanding a neuron's intrinsic properties.

Like dendritic arbor structure, a spine's morphology can impact its function. As previously discussed in chapter one, the shape and biochemical components of dendritic spines play an important role in synaptic plasticity. Spine structures can be quite diverse, but are typically categorized into four basic groups: mushroom, thin, stubby, and branched (Fig 3.1b); these categories may also reflect their functional history [6]. These categories are based on the ratio of two measurements, 1) spine neck length, and 2) head volume. Synaptic activity can alter spine shape, composition of the resident PSD, and signaling dynamics. The spine neck acts as a diffusion barrier, isolating spine heads from the parent dendritic shaft. This isolation results in a specialized biochemical compartment capable of influencing plasticity at the synapse [2]. Furthermore, though spine necks are not able to sufficiently restrict synaptic currents, neck resistance can establish a membrane potential microdomain within the spine head and specifically restrict Ca^{2+} concentrations [7-9].

The structure of dendritic arbors and spine necks may serve somewhat distinct functions, however their development and activity dynamically impact each other. In fact, the growth and development of dendritic arbors are concurrent in time and space with synaptic formation, with proteins of the postsynaptic density playing an integral role in both processes [10]. Given the likely role of Densin in synaptic plasticity, synaptogenesis, and signaling and adhesion complexes, I undertook a comparative study to measure changes in dendritic arborization and spine shape between wild type and knockout animals. Results from these studies are presented here.

Material and Methods

3.1 Infection of Primary Hippocampal Neurons and Analysis of Dendritic Arbors

Primary hippocampal cultures were prepared and maintained as described (Chapter 4.2). At 18-19 DIV cells were infected with a sindbis virus containing green fluorescent protein (GFP) as previously described [11]. 12-14 hours post-infection, cells were fixed on coverslips and mounted as described (Chapter 4.2).

Images were taken on a LSM 5 PASCAL/ Exciter confocal microscope maintained by the Caltech Biological Imaging Center. Images were acquired using a 40x/ 1.3 Plan-Apochromat oil objective. The pinhole aperture was set at 0.5 μm with a zoom of 1x and image size of 1024 x 1024.

Sholl analysis was performed using the NIH ImageJ Sholl Analysis Plugin (v1.0) downloaded from the Ghosh lab website (http://www-biology.ucsd.edu/labs/ghosh/software/). Background dendrites extending into the image view from neighboring neurons were manually deleted. The origin of the concentric radii was set at the midpoint of the longest axis of the soma. Analysis parameters were as follows: starting radius, 1 μm; ending radius, 75 μm; radius step size, 2 μm; radius span, 1 μm; span type, median. Statistics were performed using the Prism statistical package (GraphPad, San Diego, CA).

3.2 Mouse Strains and Imaging of Spines

Homozygous green fluorescent protein (GFP) line-M transgenic mice [12] in a C57BL6 background (a kind gift from Dr. Joshua Sanes, Harvard University, Cambridge, MA) were crossed with F2 generation Densin$^{+/-}$ animals to produce GFP$^{+/-}$ / Densin$^{+/-}$ animals. GFP$^{+/-}$ / Densin$^{+/-}$ animals were subsequently crossed to produce GFP expression in a Densin null mutant background. Genomic DNA was isolated from mouse ear punch or tail samples and used for PCR. Genotyping protocols for GFP line-M were previously described [12].

Four GFP positive Densin$^{+/+}$ and Densin$^{-/-}$ 8-10 week old age-matched pairs were perfused transcardially as previously described [13]. 50μm coronoal sections were cut with a vibratome and mounted with Prolong Gold antifade reagent. Slides were individually coded by a member of the Kennedy lab and randomly ordered for image acquisition. Images were acquired on a LSM 5 PASCAL/ Exciter confocal microscope with a 100x 1.4 NA lense and 2x optical zoom. Images of dendrites (from 20 sections per animal) were reconstituted from stacks of 40 0.4 μm optical sections and preprocessed with blind iterative deconvolution software (Autodeblur) Autoquant. Spine morphology was analyzed using 3DMA spine analysis software developed in the laboratory of Brent Lindquist (Stony Brook University, Stony Brook, NY) (Koh et al., 2002). By using a geometric approach, the 3DMA software automatically detects and quantifies the three-dimensional structure of dendritic spines from stacks of high-resolution confocal microscopic images. The software then assigns the detected spines to one of three morphological categories (thin, stubby, or mushroom) based on the ratio of

neck length to head volume [14]. The investigator was blind to genotype during image acquisition and analysis of spine morphology.

3.3 Statistics

Raw data are presented as averages +/- standard error of the mean (SEM), with *n* indicating the number of experiments. Data sets that report percentage changes from control values are expressed as geometric means (GM) to avoid a statistical phenomenon in which the averages of ratios tend to overestimate differences. The GM was calculated as the *n*th root of the product of the percentage changes from the control values. The standard error of the geometric mean (SEGM) was calculated by multiplying the GM by the SE of the arithmetic mean of the logarithms of the percentage changes from the control values.

Statistical analyses of two groups were measured using Student's t tests (two-tailed). One-sample t tests (two-tailed) were used to determine whether data sets that were normalized to matched control values were significantly different from 100%. Statistical analyses of data containing more than two groups were performed using the one-way ANOVA test, followed by Tukey–Kramer analysis, to account for multiple comparisons. The Kolmogorov–Smirnov method was used to assess whether data sets had Gaussian distributions, as required for t tests and ANOVA analyses. In cases where the data were not Gaussian, nonparametric tests were used as stated.

Results

3.4 Dendritic Arborization

Analysis of dendritic arbor structure in Densin ko mice revealed an effect of deletion of Densin on branching of proximal dendrites and on overall dendritic branch complexity. Qualitative observations suggested that the primary dendritic trunks emanating from the soma are thicker in Densin$^{-/-}$ hippocampal neurons. Furthermore, somal apexes from which the dendritic trunk and branches sprout are broad and flattened relative to wt neurons.

Quantitative analysis of the structure of dendritic arbors using the Sholl method revealed a statistically significant increase in the number of proximal dendrites within 10 μm of the soma (wt= 53.57 +/-1.74, ko= 103 +/-1.49; $p<0.0001$). However, the Densin ko neurons show an overall decrease in the number of dendritic branches and complexity as determined by the average number of total dendritic intersections (wt= 360.86 +/-2.15, ko= 252.82 +/-1.36; $p<0.0001$). The findings indicate that the ability to initiate branch points and extend dendrites is altered in Densin ko neurons.

3.5 CA1 Dendritic Spine Structure

The results of Quitsch et al. [15] in cultured neurons demonstrated that overexpression of Densin in primary hippocampal cultures resulted in the elaboration of the dendritic arbor structure. Furthermore, they showed that presynaptic clusters for synaptophysin formed along the elaborated dendritic branches, suggesting that Densin plays a role in synaptogenesis. This would suggest that neurons of Densin knockout animals might have a decreased spine density. To test this hypothesis, we crossed

Densin$^{-/-}$ animals with GFP+ line-M transgenic mice. These mice express GFP sparsely in a golgi-like pattern in CA1 pyramidal neurons [12]. We acquired confocal images of fluorescent basal dendrites of CA1 pyramidal neurons in littermates, with the investigator being blind to the genotype of the animal. Three-dimensional images of the dendrites were deconvolved from z-stacks, and spine morphology was analyzed as described in Section 3.2 and 3.3.

We found that adult hippocampal neurons from Densin$^{-/-}$ mice had a 13% increase in spine density compared to wild type neurons (Fig 3.3). Furthermore, the volume of spines heads decreased 11% in Densin$^{-/-}$ mice (Fig 3.3). Though a trend towards an increase in spine length was observed, the difference was not statistically significant. These results show that Densin plays a role in spine morphology and density.

References

1. Spruston, N., *Pyramidal neurons: dendritic structure and synaptic integration.* Nat Rev Neurosci, 2008. **9**(3): p. 206-21.
2. Sabatini, B.L., M. Maravall, and K. Svoboda, *Ca^{2+} signaling in dendritic spines.* Curr Opin Neurobiol, 2001. **11**(3): p. 349-56.
3. Polsky, A., B.W. Mel, and J. Schiller, *Computational subunits in thin dendrites of pyramidal cells.* Nat Neurosci, 2004. **7**(6): p. 621-7.
4. Vetter, P., A. Roth, and M. Hausser, *Propagation of action potentials in dendrites depends on dendritic morphology.* J Neurophysiol, 2001. **85**(2): p. 926-37.
5. Mainen, Z.F. and T.J. Sejnowski, *Influence of dendritic structure on firing pattern in model neocortical neurons.* Nature, 1996. **382**(6589): p. 363-6.
6. Bourne, J.N. and K.M. Harris, *Balancing structure and function at hippocampal dendritic spines.* Annu Rev Neurosci, 2008. **31**: p. 47-67.
7. Yasuda, R., et al., *Imaging calcium concentration dynamics in small neuronal compartments.* Sci STKE, 2004. **2004**(219): p. pl5.
8. Wilson, C.J., *Passive cable properties of dendritic spines and spiny neurons.* J Neurosci, 1984. **4**(1): p. 281-97.
9. Noguchi, J., et al., *Spine-neck geometry determines NMDA receptor-dependent Ca2+ signaling in dendrites.* Neuron, 2005. **46**(4): p. 609-22.
10. Cline, H. and K. Haas, *The regulation of dendritic arbor development and plasticity by glutamatergic synaptic input: a review of the synaptotrophic hypothesis.* J Physiol, 2008. **586**(6): p. 1509-17.
11. Vazquez, L.E., et al., *SynGAP regulates spine formation.* J. Neurosci., 2004. **24**: p. 8796-8805.
12. Feng, G., et al., *Imaging neuronal subsets in transgenic mice expressing multiple spectral variants of GFP.* Neuron, 2000. **28**(1): p. 41-51.
13. Carlisle, H.J., et al., *SynGAP regulates steady-state and activity-dependent phosphorylation of cofilin.* J. Neurosci., 2008. **28**: p. 13649-13683.
14. Koh, I.Y., et al., *An image analysis algorithm for dendritic spines.* Neural Comput, 2002. **14**(6): p. 1283-310.
15. Quitsch, A., et al., *Postsynaptic shank antagonizes dendrite branching induced by the leucine-rich repeat protein Densin-180.* J Neurosci, 2005. **25**(2): p. 479-87.

Figure 3.1 The morphologies of dendrites and spines affect their function. (A) Diversity of arbor structures between and within neuron classes dynamically affect their integration and propagation of action potentials, and ultimately their firing patterns. Top, dendritic morphologies of nonpyramidal cells. Left to right, fast spiking basket cell, late-spiking neurogliaform, non-fast spiking somatostatin Martinotti cell, non-fast spiking cholecystokinin (CCK) large basket cell, non-fast spiking small basket cell, and non-fast spiking double bouquet cell (adapted from Kawaguchi et al., 2006). Bottom, structures of pyramidal neurons from different cortical layers. Left to right, neurons of layer II/ III, layer V, CA3, CA1, subiculum (adapted from Spruston, 2008). (B) Structural diversity in spine size and shape. A 3-dimentional reconstruction of a dendritic shaft (gray) and protruding spines (red, thin spine; green, stubby; blue, mushroom; yellow, branched). Postsynaptic densities can also vary in shape and size (purple).

A

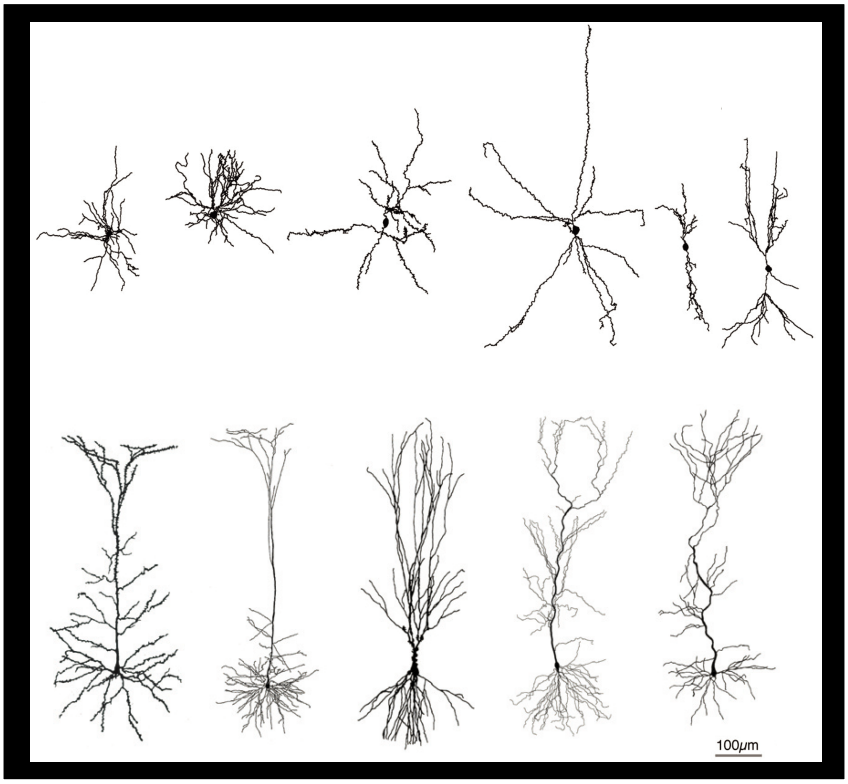
100μm

B

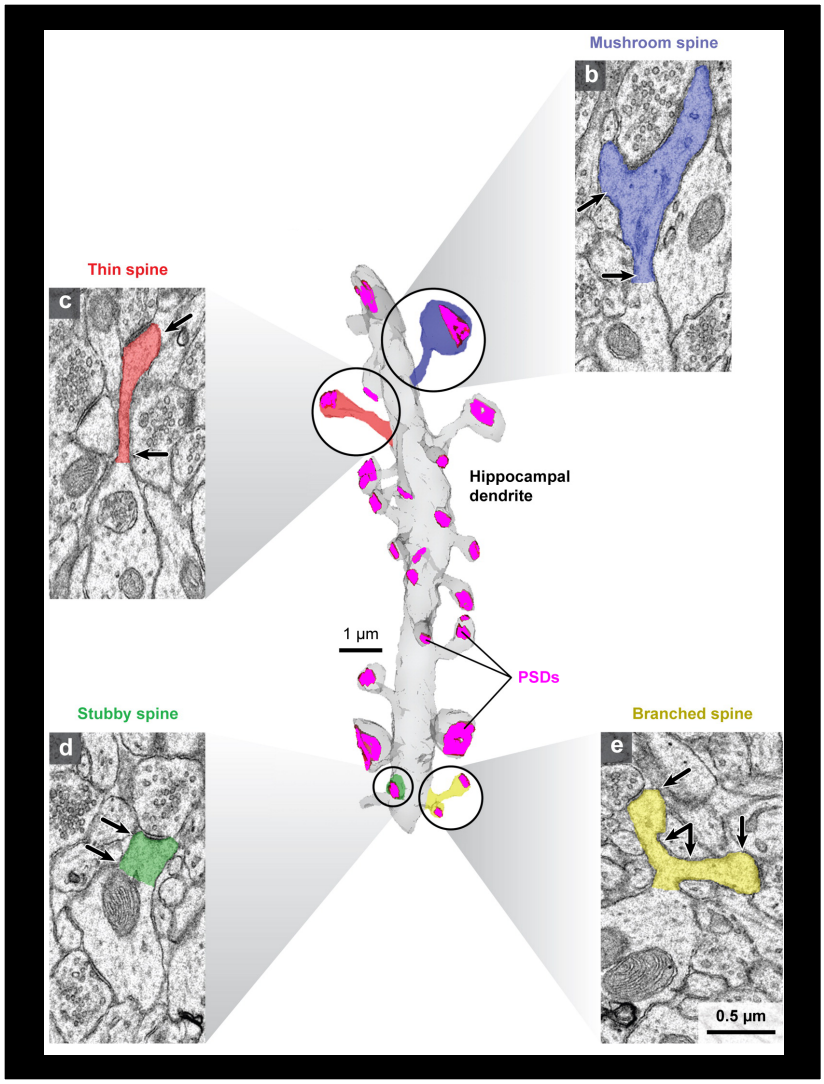
Mushroom spine
b
Thin spine
c
Hippocampal dendrite
1 μm
PSDs
Stubby spine
d
Branched spine
e
0.5 μm

Figure 3.2 Cultured Densin ko neurons have thicker dendritic trunks and an increase in the number of proximal dendritic branches. (A) 18 DIV primary hippocampal cultures infected with sindbis-GFP. Primary apical and basal dendritic trunks (arrows) are thicker in ko neurons. Images represent the phenotypic range observed. Images are compressed z-stacks of three .5 μm consecutive optical sections. (B) Sholl analysis of cultured wild type (black) and ko (red) hippocampal neurons demonstrates an increased number of proximal dendritic branches within 10 μm of the soma as determined by the average of number of intersecting dendrites (wt= 53.57 +/-1.74, ko= 103 +/-1.49; $p<0.0001$). However, Densin ko neurons exhibit a decreased level of dendritic complexity as determined by the average number of total dendritic intersections (wt= 360.86 +/-2.15, ko= 252.82 +/-1.36; $p<0.0001$). The number of dendrities crossing concentric circles of increasing radii centered about the soma was counted. Ten neurons from each of three sets of wt/ ko primary hippocampal cultures were analyzed. The x-axis indicates distance from the origin in μm; the y-axis indicates the number of dendritic intersections. Error bars indicate SEM.

A

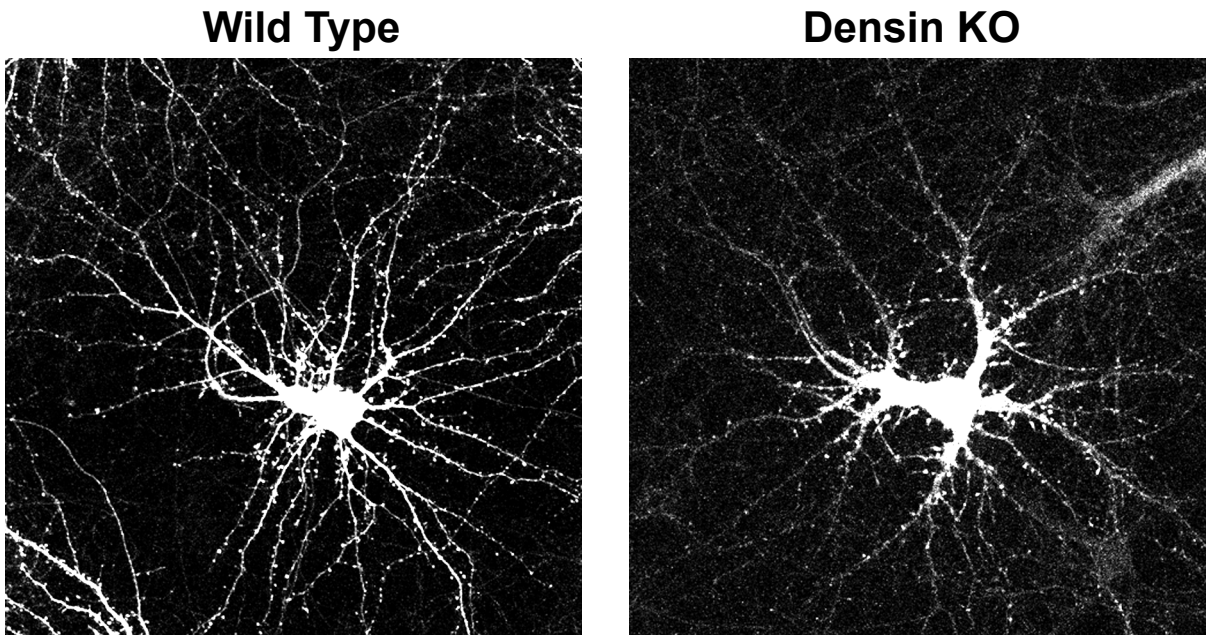
Wild Type
Densin KO

B

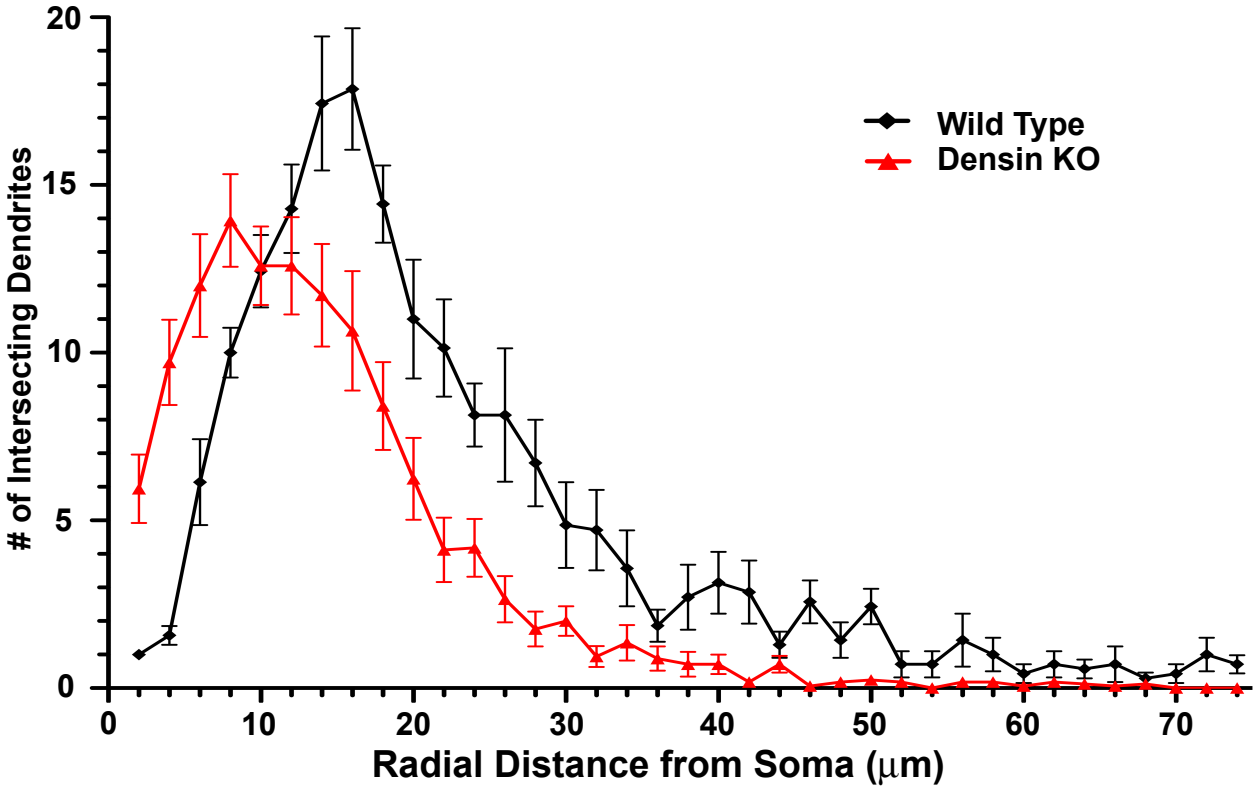
Wild Type
Densin KO
# of Intersecting Dendrites
Radial Distance from Soma (μm)
0
5
10
15
20
0
10
20
30
40
50
60
70

Figure 3.3 Homozygous deletion of Densin increases spine density and decreases spine volume on adult hippocampal CA1 neurons *in vivo*. A) Example dendrites are shown for GFP+/ Densin$^{+/+}$ and GFP+/ Densin$^{-/-}$ mice. B) The data show a significant increase in the absolute density of spines per micrometer of dendrite on Densin$^{-/-}$ hippocampal neurons compared to wildtype (wt= 1.93 +/-0.07 spines/ μm dendrite; Densin$^{-/-}$= 2.19 +/- 0.07 spines/ μm dendrite; $p<0.01$). The data also show a significant decrease in the volume of spine heads on dendrites of Densin$^{-/-}$ hippocampal neurons compared to wild type (wt= 0.067 +/- 0.002 μm^3; Densin$^{-/-}$= 0.061 +/- 0.002 μm^3; $p<0.01$). Finally, the data show no significant change in the length of spines in Densin$^{-/-}$ hippocampal neurons compared to wild type (wt= 0.59 +/-0.01 μm; Densin$^{-/-}$= 0.61 +/-0.01μm; $p>0.05$).

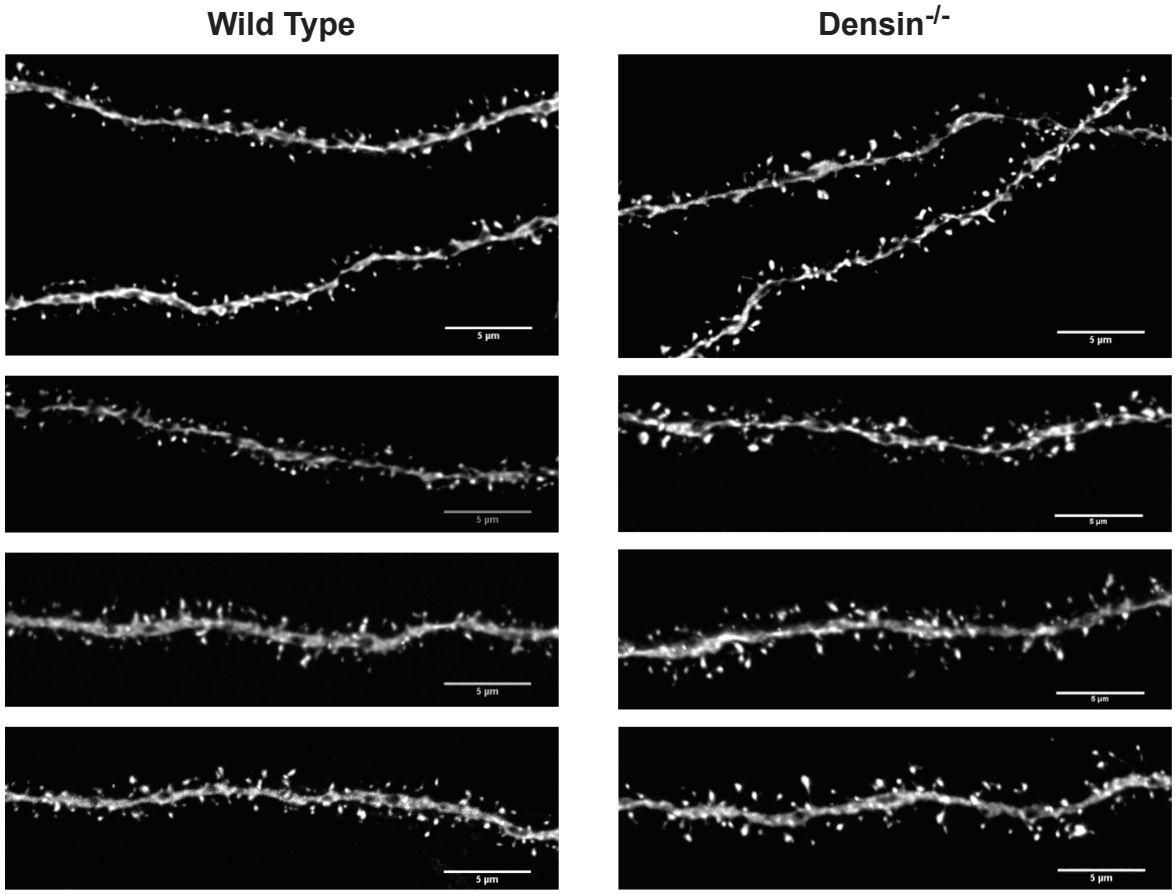
Wild Type
Densin-/-
5 µm

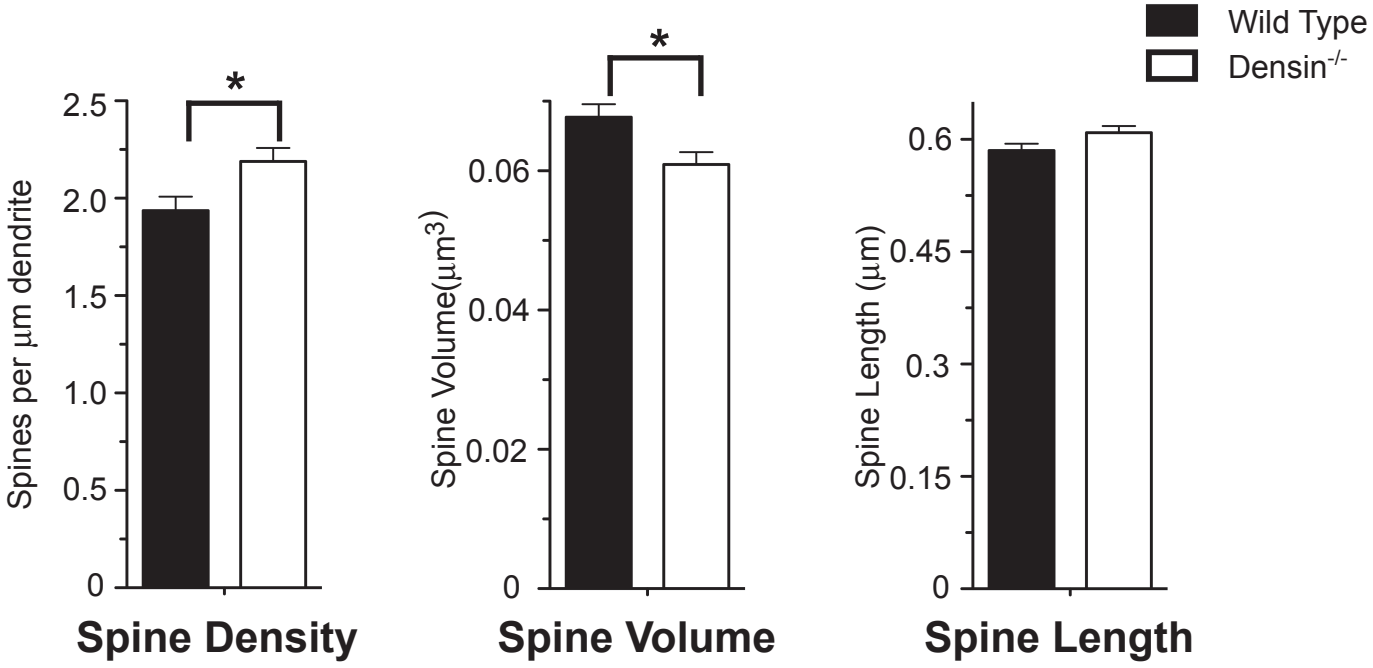
Wild Type
Densin-/-
Spines per µm dendrite
2.5
2.0
1.5
1.0
0.5
0
*
Spine Density
Spine Volume(µm3)
0.06
0.04
0.02
0
*
Spine Volume
Spine Length (µm)
0.6
0.45
0.3
0.15
0
Spine Length